

Shock Ignition of Thermonuclear Fuel with High Areal Densities

The energy gain¹ G of a direct-drive implosion is defined as the ratio between the thermonuclear energy yield and the laser energy on target. The gain is directly related to the capsule implosion velocity $G = (1/V_I^2)\eta_h\theta E_f/m_i$, where V_I is the implosion velocity, $\eta_h = E_K/E_L$ is the hydrodynamic efficiency representing the ratio between the shell kinetic energy and the laser energy on target, $E_f = 17.6$ MeV is the energy of the fusion products for a DT fusion reaction, and $m_i = 2.5 m_H$ is the average ion mass. The function θ represents the fraction of burned fuel depending on the fuel areal density $\rho R \equiv \int_0^R \rho dr$. The function $\theta = \theta(\rho R)$ is commonly approximated¹ by $\theta \approx (1 + 7/\rho R)^{-1}$, where ρR is given in g/cm². The hydrodynamic efficiency of direct-drive implosions scales² as $\eta_h \sim V_I^{0.75}/I_L^{0.25}\lambda_L^{0.5}$, where I_L is the laser intensity on target and λ_L is the laser wavelength. It follows that the target gain scales as $G \sim 1/V_I^{1.25}$, indicating that high gains require low-velocity implosions. This is because low velocities are achieved by imploding massive shells and compressing large amounts of thermonuclear fuel. Since the areal densities are approximately independent of the implosion velocities,² the burn-up fraction depends only on the laser energy and fuel adiabat. Thus, low-velocity implosions of massive shells lead to high gains, provided that the fuel is ignited. However, the energy required to trigger ignition grows rapidly as the implosion velocity decreases. As shown in Ref. 3, the shell kinetic energy required for ignition scales as $E_K^{\text{ign}} \sim 1/V_I^6$ and low-velocity implosions fail to ignite at moderate driver energies. Large lasers in the 1-MJ energy range, such as at the National Ignition Facility, are expected to ignite relatively thin shells (initial aspect ratio ~ 5) driven at high velocities, $\sim 4 \times 10^7$ cm/s, to achieve moderate gains of ~ 40 (Ref. 4). The performance of such implosions is sensitive to the growth of the Rayleigh–Taylor (RT) instability on the ablation front. The RT modes that can cause shell breakup during the acceleration phase have an inverse wave number $1/k$ comparable to the in-flight shell thickness $d(kd \sim 1)$. The number of e -foldings of growth for such modes is about $\sqrt{\text{IFAR}}$, where IFAR is the in-flight aspect ratio, which scales¹ as $\sim V^2/\alpha^{0.6}I_L^{0.27}$.

The parameter α represents the shell's in-flight adiabat defined as the ratio of the pressure to the Fermi pressure of

a degenerate electron gas. For a fully ionized DT plasma, the adiabat is given by $\alpha = P(\text{Mb})/2.3\rho(\text{g/cc})^{5/3}$. To maximize the burn-up fraction (and the areal density), the adiabat must be kept low. It follows that the shell stability can be improved by lowering the IFAR through reducing the implosion velocity. Low-velocity implosions with low IFAR's have good stability properties during the acceleration phase. However, despite their good stability properties and potential for high gains, slow targets would fail to ignite for moderate driver energies because the hot-spot temperature and pressures are too low. For example, ignition at implosion velocities of $\sim 2 \times 10^7$ cm/s and adiabats of $\alpha \sim 1$ require large multimegajoule laser drivers.

Here we show that a spherically convergent shock wave propagating through the shell during the coasting phase of the implosion enhances the compression of the hot spot, thus significantly improving the ignition conditions.⁵ The ignitor shock is launched at the end of the laser pulse and must collide with the return shock near the inner shell surface. The return shock is the shock wave driven by the hot-spot pressure propagating outward through the shell. After the ignitor and return shock collide, a third shock wave, resulting from the collision, propagates inward, leading to further compression of the hot spot. The final fuel assembly develops a peaked pressure profile with its maximum in the center. Such non-isobaric assemblies exhibit a lower ignition threshold than standard isobaric ones.⁵ This mechanism is effective only in thick-shell implosions, where the ignitor shock wave significantly increases its strength as it propagates through the converging shell.

This effect can be observed in simulations of realistic ICF implosions of thick shells like the one in Fig. 112.33 showing a thick wetted-foam shell with an outer radius of 852 μm , a 106- μm -thick layer of wetted foam CH(DT)₆, and a 240- μm -thick layer of DT ice. The initial shell aspect ratio (average shell radius/thickness) is about 2. One-dimensional simulations of a direct-drive implosion of such shells are carried out for the two 350-kJ, $\lambda_L = 0.35\text{-}\mu\text{m}$ laser pulses shown in Fig. 112.34. The dashed curve represents a standard laser pulse, while the solid curve represents a shock-ignition laser pulse with a power

spike at the end of the pulse used to drive the ignitor shock. Both laser pulses use an intensity picket at the beginning of the pulse to shape the adiabat profile and to improve the target stability. The in-flight adiabat of the shell is $\alpha \approx 1$, the implosion velocity is $V = 2.5 \times 10^7$ cm/s, and the IFAR ≈ 17 . The ultralow IFAR indicates that the integrity of the shell is not significantly affected by the Rayleigh–Taylor instability. The simulation of the implosions for the two laser pulses is carried out using the hydrocode *LILAC*. Figure 112.35 compares the pressure and density profiles at the time of peak compression for the standard pulse shape (dashed) and the shock-ignition pulse shape (solid). Notice that the hot-spot pressure for the

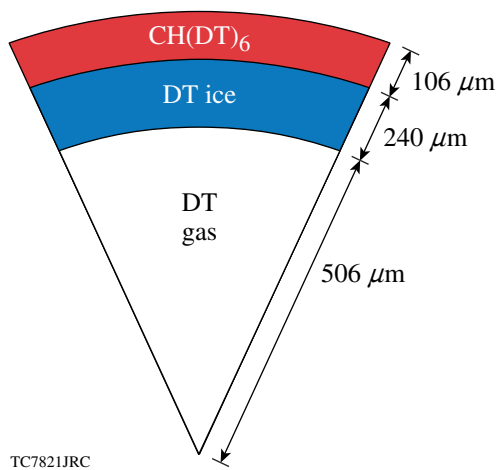


Figure 112.33
Thick wetted-foam target used in the shock-ignition simulations.

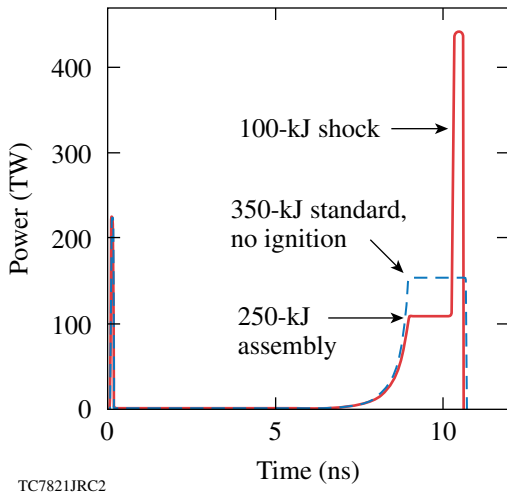


Figure 112.34
UV 350-kJ standard pulse shape (dashed) and shock-ignition pulse shape (solid).

shock-ignition pulse shape is about twice as high as for the standard pulse shape. While the target driven by the standard pulse is far from ignition, the shock-ignited target is at marginal ignition. Marginal ignition for a shock-ignited target is estimated by the size of the shock-launching-time ignition window, i.e., the time interval during which the ignitor shock needs to be launched to trigger ignition. If the ignition window is very narrow (only tens of picoseconds), the shock-ignited target is close to marginal ignition. To exceed the marginal ignition conditions and to widen the ignition window, the total laser energy needs to be increased.

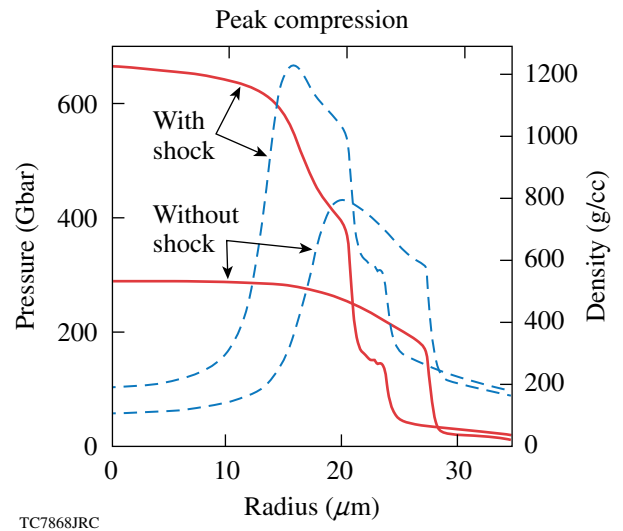


Figure 112.35
Density (dashed) and pressure (solid) profiles at peak compression for the standard and shock-ignition pulse shape.

Since the laser intensity during the power spike is considerably higher than during the assembly pulse, hot electrons can be generated in the corona by laser–plasma instabilities. In standard implosions, hot electrons can preheat the shell, thus raising the adiabat, reducing the final compression, and preventing the ignition of the hot spot. In shock ignition, hot electrons generated during the power spike may have a positive effect on the implosions. Since the areal density grows rapidly in time during the final stages of the implosion, the range of the hot electrons from the intensity spikes is less than the shell thickness. In this case, the hot electrons are stopped on the shell surface and help drive the ignitor shock. Figure 112.36 shows a plot of the laser intensity (solid curve) and the areal density evolution (dashed curve) during the power spike. Since the ρR range of 100-keV electrons in DT (about 17 mg/cm², dashed line in Fig. 112.36) is much smaller than the shell areal density (50 to 80 mg/cm²) during the spike, the hot electrons

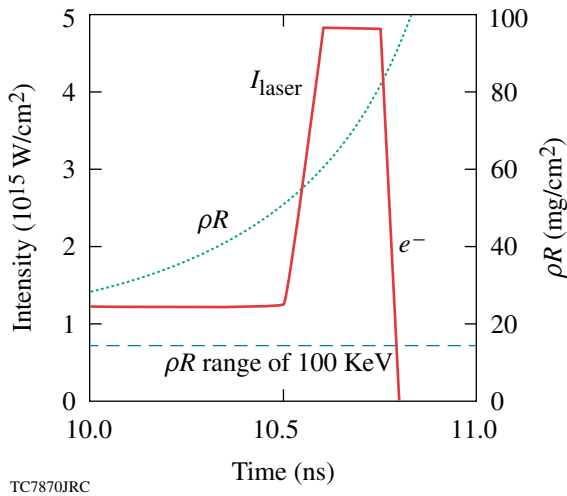


Figure 112.36 Evolution of the laser intensity (solid) and the areal density (dashed) during the power spike.

of moderate energy (~100 keV) are stopped before penetrating deep into the shell, thus augmenting the strength of the ignitor shock. The effects of hot electrons are included in the simulations through a multigroup diffusion model for the hot electrons as described in Ref. 6. In the simulations, the hot electrons are generated isotropically during the power spike in the corona with their birth temperature set at 150 keV and with a Maxwellian distribution function. The total energy into hot electrons is assumed to be 25% of the laser energy during the power spike. As shown in Fig. 112.37, the ignition window

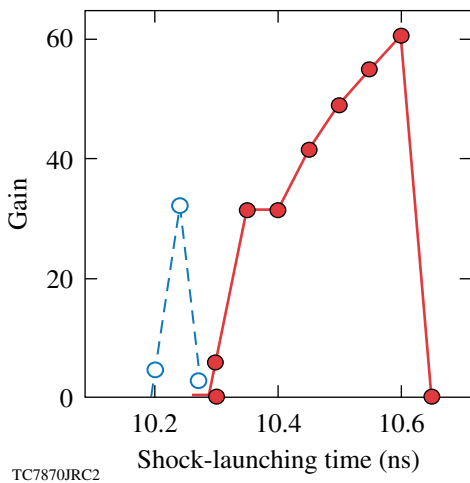


Figure 112.37 Shock-launching-time ignition window with (solid) and without (dashed) hot electrons.

is considerably wider when the effects of hot electrons are included in the simulation, thus showing that hot electrons can indeed benefit the shock-ignition scheme as long as their range does not exceed the shell thickness.

Another important effect to be included in shock-ignition targets is the long mean free path of the thermal coronal electrons heated to high temperatures during the power spike. The power spike raises the coronal electron temperatures to about 7 keV, causing the heat-carrying electrons to free-stream to the ablation front, thus enhancing heat conduction. A nonlocal heat-conduction model is, therefore, required to adequately model the electron heat transfer during the power spike. To estimate the effects of nonlocal heat transport, the model of Ref. 7 is included in the simulations of the ignitor-shock generation during the power spike. The new conditions for ignition and gain are computed in terms of the ignition window and shown in Fig. 112.38. As expected, the long-mean-free-path electrons augment the heat transfer during the power spike, thus driving a stronger ignitor shock. The ignition window is widened by nonlocal transport, and the gain is higher than without nonlocal effects.

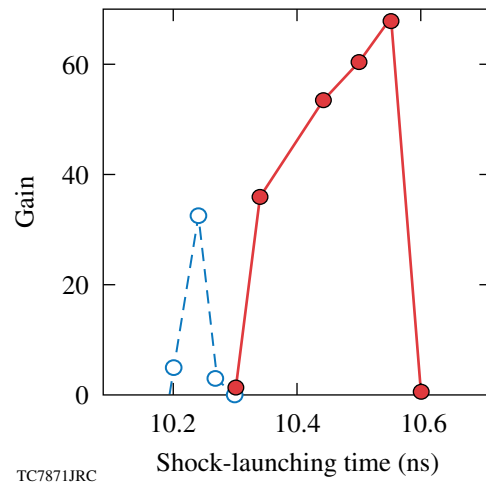


Figure 112.38 Ignition window with (solid) and without (dashed) nonlocal heat transport.

It is shown that a two-step ignition scheme can be configured by combining a fuel-assembly laser pulse and a shock-driving power spike. The ignitor shock enhances the compression of the hot spot, thus leading to a significant reduction of the energy required for ignition and high gains. A powerful laser pulse or particle beam can be used to drive the ignitor shock to trigger ignition at relatively low driver energies.

ACKNOWLEDGMENT

This work was supported by the U.S. Department of Energy Office of Fusion Energy Science and Office of Inertial Confinement Fusion under Cooperative Agreement No. DE-FC02-04ER54789 and DE-FC52-92SF19460, the University of Rochester, and the New York State Energy Research and Development Authority. The support of DOE does not constitute an endorsement by DOE of the views expressed in this article.

REFERENCES

1. J. D. Lindl, *Inertial Confinement Fusion: The Quest for Ignition and Energy Gain Using Indirect Drive* (Springer-Verlag, New York, 1998).
2. R. Betti and C. Zhou, *Phys. Plasmas* **12**, 110702 (2005).
3. M. C. Herrmann, M. Tabak, and J. D. Lindl, *Nucl. Fusion* **41**, 99 (2001).
4. P. W. McKenty, V. N. Goncharov, R. P. J. Town, S. Skupsky, R. Betti, and R. L. McCrory, *Phys. Plasmas* **8**, 2315 (2001).
5. R. Betti, C. D. Zhou, K. S. Anderson, L. J. Perkins, W. Theobald, and A. A. Solodov, *Phys. Rev. Lett.* **98**, 155001 (2007).
6. J. Delettrez and E. B. Goldman, Laboratory for Laser Energetics, University of Rochester, Rochester, NY, LLE Report No. 36 (1976).
7. G. P. Schurtz, Ph. D. Nicolaï, and M. Busquet, *Phys. Plasmas* **7**, 4238 (2000).